

Theoretical Notes

Note 357

June 1990

Time-domain analysis of one-dimensional electromagnetic scattering by  
lossy media

J.J.A. Klaasen

Electromagnetic Pulse Group

Physics and Electronics Laboratory

Netherlands Organization for Applied Scientific Research

P.O.Box 96864

2509 JG The Hague

The Netherlands

ABSTRACT

A study was performed to investigate the electromagnetic scattering in the time domain by a plane interface between two half-spaces. One half-space is assumed to be vacuum, while the other half-space is homogeneous and consists of lossy material. The incident field is assumed to be a uniform plane wave. Hence, this study addresses the one-dimensional scattering problem. For brevity, only the case of horizontal polarization is presented.

Starting with the equations for the reflected and transmitted waves in the  $s$ - or Laplace-domain, corresponding time-domain expressions are obtained by decomposing the  $s$ -domain expressions in such a way that standard Laplace transforms can be recognized. The resulting time-domain expressions are in closed form, i.e., are given in terms of elementary functions or integrals of elementary functions.

Numerical results are presented for the scattering of a unit-step function and a Nuclear ElectroMagnetic Pulse (NEMP) using the derived time-domain expressions. The numerical implementation uses a time-marching procedure.

## Table of Contents

Section		Page
1	INTRODUCTION	3
2	DESCRIPTION AND SOLUTION OF THE ELECTROMAGNETIC SCATTERING PROBLEM IN THE LAPLACE DOMAIN	4
	2.1 Description of the scattering configuration	4
	2.2 Solution of the scattering problem in the Laplace domain	6
3	TIME-DOMAIN SOLUTION FOR A UNIT-STEP INCIDENT FIELD	10
	3.1 Transmitted electric field	10
	3.2 Transmitted magnetic fields	18
	3.3 Reflected fields	19
4	NUMERICAL RESULTS	21
	4.1 Numerical implementation	21
	4.2 Unit-step incident field	22
	4.3 NEMP incident field	25
5	CONCLUSIONS	29
6	REFERENCES	30
APPENDICES		
A	THE LATE-TIME BEHAVIOR OF THE FIELD QUANTITIES	31
B	STANDARD LAPLACE TRANSFORMS OF SOME BESSEL FUNCTIONS	36
C	RESPONSE TO WAVEFORMS OTHER THAN THE UNIT-STEP FUNCTION	37

## 1 INTRODUCTION

In many electromagnetic coupling problems, the influence of the earth has to be taken into account, because an object in the vicinity of the earth's surface is not only irradiated by the incident field, but also by the field reflected by the earth. Such is the case, amongst others, in Nuclear ElectroMagnetic Pulse (NEMP) interaction studies in which time-domain results are desirable. Therefore, a study was performed to investigate the scattering of a plane wave by a plane interface between two half-spaces in the time domain.

One of the most well-known methods to obtain time-domain results is to compute the response for many frequencies, after which a numerical inverse Fast Fourier Transform (FFT) is applied. In this report exact, analytical time-domain expressions are obtained by using standard Laplace transforms found in many textbooks. An other approach was taken by Leuthäuser [6], who obtained time-domain expressions by complex contour integration in the complex  $\omega$ -plane.

The waveform of the incident field is taken as a unit-step function. The resulting unit-step response is in closed form, i.e., is given in terms of elementary functions or integrals of elementary functions. In Appendix C a method is presented to obtain the response to any waveform other than the unit-step function. This method typically involves a convolution integral.

For brevity, this Note presents the results for horizontally polarized incident fields only. Results for vertical polarization can be obtained using the same techniques (See Klaasen [3]). In Chapter 2 the scattering configuration is presented and the solution of the scattering problem is presented in the Laplace domain for horizontally polarized incident fields. In Chapter 3 the Laplace-domain expressions of Chapter 2 are transformed back to the time domain. To illustrate the outlined procedure, the reflected and transmitted electromagnetic fields of a unit-step function and of a NEMP are determined in Chapter 4. Finally, conclusions are drawn in Chapter 5.

## 2 DESCRIPTION AND SOLUTION OF THE ELECTROMAGNETIC SCATTERING PROBLEM IN THE LAPLACE DOMAIN

In Section 2.1 the scattering configuration is described, and in Section 2.2 the solution of the scattering problem is presented in the Laplace domain. In later chapters the Laplace-domain expressions given in Section 2.2 are used to obtain the time-domain expressions.

Because the material presented in this Chapter is well-known and can be found in almost any textbook about electromagnetic scattering, see Stratton [8], it is sketchy and serves merely as an introduction to the forthcoming chapters.

### 2.1 Description of the scattering configuration

The one-dimensional scattering configuration depicted in Fig. 2.1 is considered. To specify the position in this unbounded space, we employ the coordinates  $(x, y, z)$  with respect to a fixed, orthonormal, right-handed, Cartesian reference frame with origin  $O$ . The base vectors along the axes are denoted by  $\underline{i}_x$ ,  $\underline{i}_y$  and  $\underline{i}_z$ . Then the position vector in this coordinate system is given by

$$\underline{r} = x\underline{i}_x + y\underline{i}_y + z\underline{i}_z. \quad (2.1)$$

The time coordinate is denoted by  $t$ , with  $t \in \mathbb{R}$ . Let the Laplace transform of  $f(t)$  be denoted by  $\hat{f}(s)$ . Then  $f(t)$  and  $\hat{f}(s)$  are related by the Laplace transform with respect to time, defined by

$$\mathcal{L}\{f(t)\} = \hat{f}(s) = \int_0^{\infty} e^{-st} f(t) dt, \quad (2.2)$$

while the inverse Laplace transform is given by

$$f(t) = \frac{1}{2\pi i} \int_{\alpha-i\infty}^{\alpha+i\infty} e^{st} \hat{f}(s) ds, \quad (2.3)$$

where  $i$  is the imaginary unit, and  $s$  denotes the complex frequency. The

integration is performed along the Bromwich contour, LePage [5], i.e., if  $t > 0$  the path of integration is closed with a semicircle of infinite radius in the left half-plane of the  $s$ -plane and, if  $t < 0$ , with a semicircle in the right half-plane. The positive real number  $\alpha$  which occurs in Eq.(2.3) is chosen such that all singularities lie to the left of the line  $\alpha - i\infty, \alpha + i\infty$ . This ensures a causal solution for  $f(t)$ . More details can be found in Appendix A.

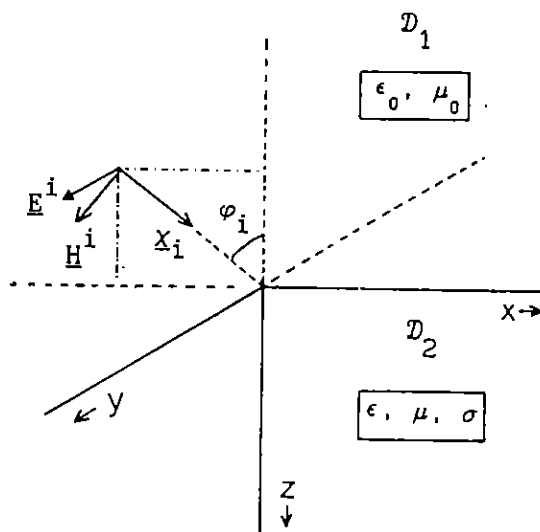


Fig. 2.1. Electromagnetic scattering configuration.

Let the half-space  $\mathcal{D}_1$  be given by

$$\mathcal{D}_1 = \{ x, y, z \in \mathbb{R} \mid z < 0 \}, \quad (2.4)$$

and let the half-space  $\mathcal{D}_2$  be given by

$$\mathcal{D}_2 = \{ x, y, z \in \mathbb{R} \mid z > 0 \}. \quad (2.5)$$

This configuration is irradiated by an incident uniform electromagnetic plane wave with horizontal polarization, i.e., the electric field has a

component in the y-direction only. The source which generates the incident field is located in  $\mathcal{D}_1$ . The constitutive constants of the half-space  $\mathcal{D}_1$  are assumed to be those of vacuum, i.e.,  $\epsilon_0$  and  $\mu_0$ . The half-space  $\mathcal{D}_2$  is assumed to consist of homogeneous, isotropic, time-invariant and linear material. Furthermore, the material in  $\mathcal{D}_2$  is instantaneous and locally reacting, and it is characterized in its electromagnetic behavior by the permittivity  $\epsilon$ , the permeability  $\mu$ , and the electrical conductivity  $\sigma$ . Furthermore, there are no sources present in  $\mathcal{D}_2$ .

The incident wave propagates in the direction of the propagation vector  $\underline{x}_i$ . The propagation vector  $\underline{x}_i$  is of unit length, i.e.,  $\|\underline{x}_i\| = 1$ , and makes an angle  $\varphi_i$  with the normal  $\underline{n}$  on the plane interface between the two media, with  $\varphi_i < 90^\circ$ . The vector  $\underline{n}$  is also of unit length, and is directed inwards  $\mathcal{D}_2$ .

## 2.2 Solution of the scattering problem in the Laplace domain

At  $t = 0$  the incident field hits the interface between  $\mathcal{D}_1$  and  $\mathcal{D}_2$  at  $\underline{r} = \underline{0}$ . Then the incident electric field is given by

$$\hat{E}_y^i(\underline{r}, s) = \hat{E}_0(s) e^{-\gamma_0(\underline{x}_i \cdot \underline{r})}, \quad \underline{r} \in \mathcal{D}_1 \quad (2.6)$$

in which  $\underline{x}_i$  denotes the propagation vector given by

$$\underline{x}_i = \sin \varphi_i \hat{i}_x + \cos \varphi_i \hat{i}_z. \quad (2.7)$$

In Eq.(2.6),  $\gamma_0$  denotes the propagation constant given by

$$\gamma_0 = s (\epsilon_0 \mu_0)^{1/2} = \frac{s}{c}, \quad (2.8)$$

in which  $c$  denotes the speed of light in vacuum. In Eq.(2.6),  $\hat{E}_0(s)$  denotes the Laplace transform of the waveform of the incident electric field.

The incident magnetic field follows from Maxwell's equations and is given by

$$\begin{aligned}\hat{H}_x^i(\underline{r}, s) &= -\cos \varphi_i Y_0 \hat{E}_y^i, \\ \hat{H}_z^i(\underline{r}, s) &= \sin \varphi_i Y_0 \hat{E}_y^i,\end{aligned}\quad \underline{r} \in \mathcal{D}_1 \quad (2.9)$$

where  $Y_0$  denotes the wave admittance of vacuum given by

$$Y_0 = \hat{H}_0 / \hat{E}_0 = \left( \frac{\epsilon_0}{\mu_0} \right)^{1/2}. \quad (2.10)$$

The propagation constant of the transmitted fields in  $\mathcal{D}_2$  is given by

$$\underline{\gamma} = \|\underline{\gamma}\| = (s\mu(s\epsilon + \sigma))^{1/2}, \quad (2.11)$$

where  $\underline{\gamma}$  is given by

$$\underline{\gamma} = \gamma_x \underline{i}_x + \gamma_z \underline{i}_z, \quad (2.12)$$

in which

$$\begin{aligned}\gamma_x &= \gamma_0 \sin \varphi_i, \\ \gamma_z &= \sqrt{\gamma^2 - \gamma_x^2}.\end{aligned}\quad (2.13)$$

Let  $v$  denote the propagation speed of the waves in  $\mathcal{D}_2$  in the lossless case, i.e.,  $\sigma = 0$ , then  $v$  is given by

$$v = \frac{1}{\sqrt{\epsilon\mu}}. \quad (2.14)$$

Subsequently, we define  $\varphi_t$  as the angle of refraction, also in the lossless case. Hence,

$$\cos \varphi_t = \sqrt{1 - \frac{v^2}{c^2} \sin^2 \varphi_i}, \quad (2.15)$$

which follows directly from Snell's law.

Using Eqs.(2.11)-(2.15), the propagation constant  $\gamma_z$  is represented as

$$\gamma_z = \frac{\cos \varphi_t}{v} \sqrt{s^2 + 2as}, \quad (2.16)$$

in which

$$a = \frac{\sigma}{2\epsilon} \cos^{-2} \varphi_t. \quad (2.17)$$

The reflected fields in  $\mathcal{D}_1$  propagate in the direction of the propagation vector  $\underline{\chi}_r = \sin \varphi_i \underline{i}_x - \cos \varphi_i \underline{i}_z$ , and are represented by

$$\begin{aligned} \hat{E}_y^r(\underline{r}, s) &= \hat{R} \hat{E}_0 e^{-\gamma_0(\underline{\chi}_r \cdot \underline{r})} = \hat{R} \hat{E}_0 e^{-s \frac{x}{c} \sin \varphi_i + s \frac{z}{c} \cos \varphi_i}, \\ \hat{H}_x^r(\underline{r}, s) &= \cos \varphi_i Y_0 \hat{E}_y^r, \\ \hat{H}_z^r(\underline{r}, s) &= \sin \varphi_i Y_0 \hat{E}_y^r, \end{aligned} \quad \underline{r} \in \mathcal{D}_1 \quad (2.18)$$

where  $\hat{R}$  denotes the reflection coefficient for horizontal polarization, and is determined from the electromagnetic boundary conditions at  $z = 0$ .  $\hat{R}$  is given by

$$\hat{R} = \frac{s - \rho \sqrt{s^2 + 2as}}{s + \rho \sqrt{s^2 + 2as}}, \quad (2.19)$$

in which

$$\rho = \sqrt{\epsilon_r / \mu_r} \frac{\cos \varphi_t}{\cos \varphi_i}. \quad (2.20)$$

Observe that for the lossless case  $\hat{R}$  yields

$$\lim_{\sigma \rightarrow 0} \hat{R} = \frac{1 - \rho}{1 + \rho}. \quad (2.21)$$



An important property of  $\rho$  is that when the angle of incidence equals the well-known Brewster angle,  $\rho = 1$ . The Brewster angle can be calculated from

$$\tan \varphi_b = \left( \frac{\mu_r (\mu_r - \epsilon_r)}{\epsilon_r \mu_r - 1} \right)^{1/2}, \quad \mu_r \geq \epsilon_r \quad (2.22)$$

Note that the Brewster angle exists only if  $\mu_r$  is larger than or equal to  $\epsilon_r$ . From Eq.(2.20), we can deduce that  $\rho$  is smaller than one, if  $\epsilon_r < \mu_r$ , and the angle of incidence  $\varphi_i$  is smaller than the Brewster angle  $\varphi_b$ .

Using the expression for  $\gamma_z$  given by Eq.(2.16), the transmitted fields in  $\mathcal{D}_2$  are expressed as

$$\begin{aligned} \hat{E}_y^t(\underline{r}, s) &= \hat{T} \hat{E}_0 e^{-(\gamma \cdot \underline{r})} = \hat{T} \hat{E}_0 e^{-\left(s \frac{x}{v} \sin \varphi_t + \frac{z}{v} \cos \varphi_t \sqrt{s^2 + 2as}\right)}, \\ \hat{H}_x^t(\underline{r}, s) &= -Y_t \hat{E}_y^t, \\ \hat{E}_z^t(\underline{r}, s) &= Y_n \hat{E}_y^t, \end{aligned} \quad \underline{r} \in \mathcal{D}_2 \quad (2.23)$$

where  $Y_n$  and  $Y_t$  denote the normal and transverse—or surface—wave impedances, respectively, and are given by

$$\begin{aligned} Y_t &= \frac{\gamma_z}{s\mu}, \\ Y_n &= \frac{\gamma_x}{s\mu}. \end{aligned} \quad (2.24)$$

$\hat{T}$  in Eq.(2.23) denotes the TE-mode transmission coefficients given by

$$\hat{T} = \frac{2s}{s + \rho \sqrt{s^2 + 2as}}. \quad (2.25)$$

### 3 TIME-DOMAIN SOLUTION FOR A UNIT-STEP INCIDENT FIELD

The Laplace-domain expressions for the transmitted and reflected fields presented in Section 2.2 are used to obtain the unit-step response in the time domain. This is done by decomposing the expressions in such a way, that standard Laplace transforms can be recognized. The procedure for obtaining the response to waveforms other than the unit-step function is described in Appendix C.

#### 3.1 Transmitted electric field

The transmitted field for the TE-mode is given by Eq.(2.23) together with Eqs.(2.24)-(2.25). Let  $U(t)$  denote the Heaviside unit-step function whose Laplace transform is given by  $s^{-1}$ , i.e.,  $\mathcal{L}\{U(t)\} = s^{-1}$ . Because we determine the unit-step response, we have that  $\hat{E}_0 = s^{-1}$ . The transmitted electric field can then be expressed as

$$\hat{E}_y^t = \frac{2}{s + \rho\sqrt{s^2+2as}} e^{-s(\underline{x}_t \cdot \underline{r})/v - \frac{z}{v} \cos \varphi_t (\sqrt{s^2+2as} - s)} \quad (3.1)$$

with  $\rho$  given by Eq.(2.20), and in which  $\underline{x}_t$  denotes the unit-vector in the direction of propagation of the transmitted field given by

$$\underline{x}_t = \sin \varphi_t \underline{i}_x + \cos \varphi_t \underline{i}_z \quad (3.2)$$

The square roots in Eq.(3.1) have branch points at  $s = 0$  and  $s = -2a$  which have to be dealt with first. To ensure that they are single valued, a branch cut is introduced. Fig. 3.1 shows the branch cut and the behavior of  $(s^2+2as)^{1/2}$  in the complex  $s$ -plane. The sign of the real part of the root has to be chosen such that a causal solution is obtained. A prerequisite for obtaining a causal solution is that  $e^{st} \hat{E}_y^t$  must vanish along the semicircle of the Bromwich contour in the right half-plane. This follows from Eq.(2.3) together with Cauchy's theorem. Then, for  $t < (\underline{x}_t \cdot \underline{r})/v$ , to the right of the line  $s = -a$ , we must have  $\text{Re}((s^2+2as)^{1/2}) > 0$ . The sign of the imaginary part is determined by the sign of the real part.

To obtain the branch cut of Fig. 3.1, we must have  $\text{Re}\{(s^2+2s)^{1/2}\} < 0$  to the left of the line  $s = -a$ . Otherwise a branch cut along the line  $s = -a$  would arise.

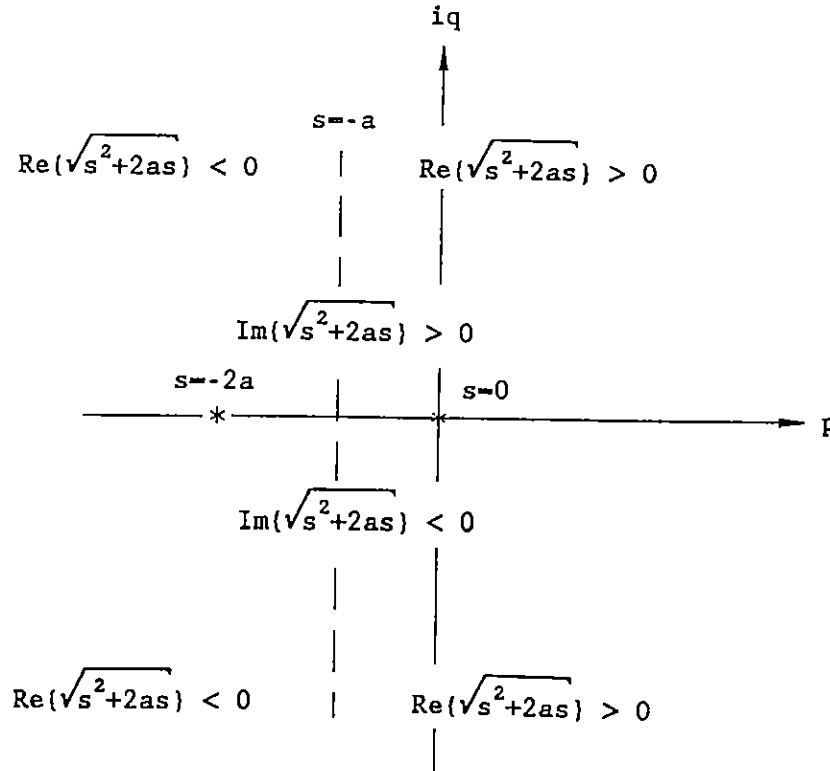


Fig. 3.1. Branch cut and behavior of  $(s^2+2as)^{1/2}$  in the complex  $s$ -plane.

Now the behavior of the complex square root is known, any poles of the transmitted field can be analyzed. The transmitted field has a pole at  $s = 0$ , and seems to have a pole at

$$s_0 = -a \frac{2\rho^2}{\rho^2 - 1} \quad \rho \neq 1 \quad (3.3)$$

But consider the case  $\rho^2 > 1$ . Then  $s_0$  is located in the left half-plane where the negative sign of the root in the denominator of Eq.(3.1) has to be chosen. Therefore, when  $\rho > 1$ ,  $s_0$  is not a pole. Subsequently, consider the case  $\rho^2 < 1$ . Now  $s_0$  is located in the right half-plane where the positive

sign of the root has to be chosen. Consequently,  $s_0$  does not represent a pole in this case either. Notice that  $s_0$  is a zero of the reflection coefficient given by Eq.(2.19). This zero supports the so-called Zenneck wave—see Barlow et al. [1].

After multiplying the denominator as well as the numerator of Eq.(3.1) by  $\rho\sqrt{s^2+2as} - s$  (notice that this term corresponds to the numerator of the reflection coefficient  $\hat{R}$ ), we obtain

$$\hat{E}_y^t = \frac{2s^{-1}}{\rho^2-1} \frac{\rho\sqrt{s^2+2as} - s}{s - s_0} e^{-s(\underline{\chi}_t \cdot \underline{r})/v - \frac{z}{v} \cos \varphi_t (\sqrt{s^2+2as} - s)}, \quad (3.4)$$

in which  $s_0$  denotes the Zenneck zero given by Eq.(3.3). Notice that the Zenneck zero of the denominator is always canceled by the numerator.

The reflected and transmitted field quantities can be expressed in terms of the functions  $\hat{f}_0$  and  $\hat{f}_1$  defined as

$$\hat{f}_0(s, \xi, z) = \left(1 + \frac{2 - \xi}{s + \xi}\right) \frac{e^{-z(\sqrt{(s+1)^2-1} - (s+1))}}{\sqrt{(s+1)^2-1}}, \quad (3.5)$$

$$\hat{f}_1(s, \xi, z) = \frac{1}{s + \xi} e^{-z(\sqrt{(s+1)^2-1} - (s+1))}$$

where  $\xi$  is a parameter to be determined later.

Using the just defined functions  $\hat{f}_0$  and  $\hat{f}_1$ , the expressions for the transmitted electric field can be represented as

$$\hat{E}_y^t = \frac{2}{\rho^2-1} e^{-z/\delta} e^{-s(\underline{\chi}_t \cdot \underline{r})/v} \left( \right. \quad (3.6)$$

$$\left. \rho \frac{1}{a} \hat{f}_0\left(\frac{s}{a}, \xi, z/\delta\right) - \frac{1}{a} \hat{f}_1\left(\frac{s}{a}, \xi, z/\delta\right) \right),$$

where  $\delta$  denotes the skin depth for the high-frequency/low-loss approximation (Klaasen [2]) given by

$$\delta = 2\epsilon v \cos \varphi_t / \sigma. \quad (3.7)$$

Furthermore, in Eq.(3.5),  $\xi$  denotes the Zenneck zero normalized by  $-a$ , given by

$$\xi = \frac{2\rho^2}{\rho^2 - 1}, \quad (3.8)$$

The functions  $\hat{f}_0$  and  $\hat{f}_1$  are ready to be transformed to the time domain using the standard Laplace transforms listed in Appendix B. After doing so, we obtain for  $f_0$  and  $f_1$

$$f_0(t, \xi, z) = \left\{ \delta(t) + (2-\xi) e^{-\xi t} \right\} * e^{-t} I_0(\sqrt{t^2+2tz}) U(t), \quad (3.9)$$

$$f_1(t, \xi, z) = e^{-\xi t} * e^{-t} \left\{ z \frac{I_1(\sqrt{t^2+2tz})}{\sqrt{t^2+2tz}} + \delta(t) \right\} U(t),$$

where we have used the property  $\mathcal{L}^{-1}(\hat{f}(s+1)) = e^{-t} f(t)$ .  $I_0$  and  $I_1$  denote the modified Bessel functions of the first kind and of order zero and one, respectively. Furthermore,  $\delta(t)$  denotes the delta function, and the asterisk denotes the convolution operator given by

$$g(t) = h(t) * f(t) = \int_0^t h(t-\tau) f(\tau) d\tau. \quad (3.10)$$

After introduction of the auxiliary functions  $h_0$ ,  $h_1$  and  $h_2$  defined by

$$\begin{aligned}
 h_0(t, \beta, z) &= e^{-\beta t} \int_0^t e^{-(1-\beta)\tau} I_0(\sqrt{\tau^2 + 2\tau z}) d\tau, \\
 h_1(t, \beta, z) &= e^{-\beta t} \left[ 1 + z \int_0^t e^{-(1-\beta)\tau} \frac{I_1(\sqrt{\tau^2 + 2\tau z})}{\sqrt{\tau^2 + 2\tau z}} d\tau \right], \\
 h_2(t, z) &= e^{-t} I_0(\sqrt{t^2 + 2tz}),
 \end{aligned} \tag{3.11}$$

and after applying the convolution operator, the expressions for  $f_0$  and  $f_1$  are represented as

$$\begin{aligned}
 f_0(t, \xi, z) &= h_2(t, z) + (2-\xi)h_0(t, \xi, z), \\
 f_1(t, \xi, z) &= h_1(t, \xi, z).
 \end{aligned} \tag{3.12}$$

The Figs. 3.2-3.4 show the functions  $h_0$ ,  $h_1$  and  $h_2$  as a function of time for different  $\beta$ .

After applying the inverse Laplace transform to Eq.(3.5) analytically, the time-domain expression for the transmitted electric field is given by

$$E_y^t(\underline{r}, t) = \frac{2}{\rho^2 - 1} U(t') e^{-z'} \left\{ \rho f_0(at', \xi, z') - f_1(at', \xi, z') \right\}, \tag{3.13}$$

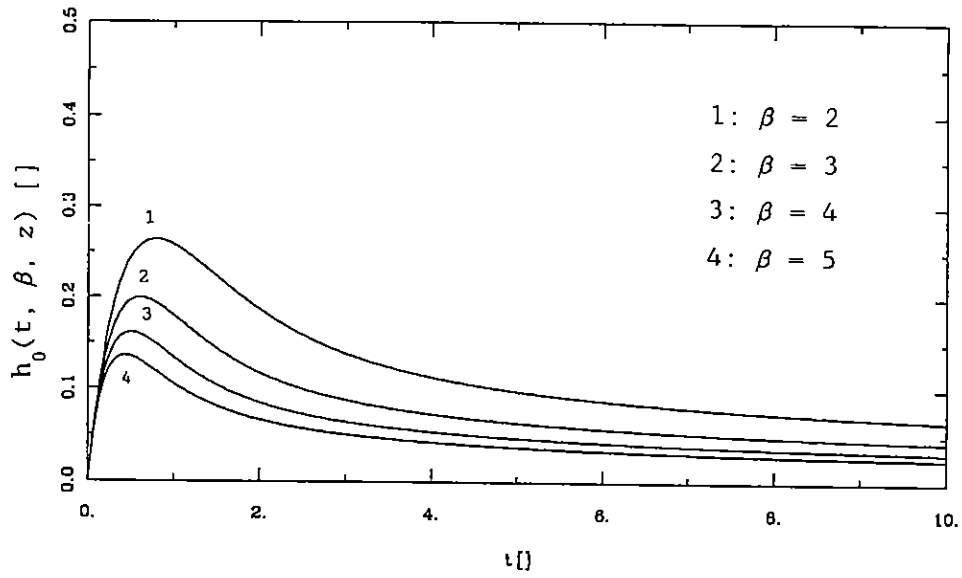
in which

$$z' = z / \delta. \tag{3.14}$$

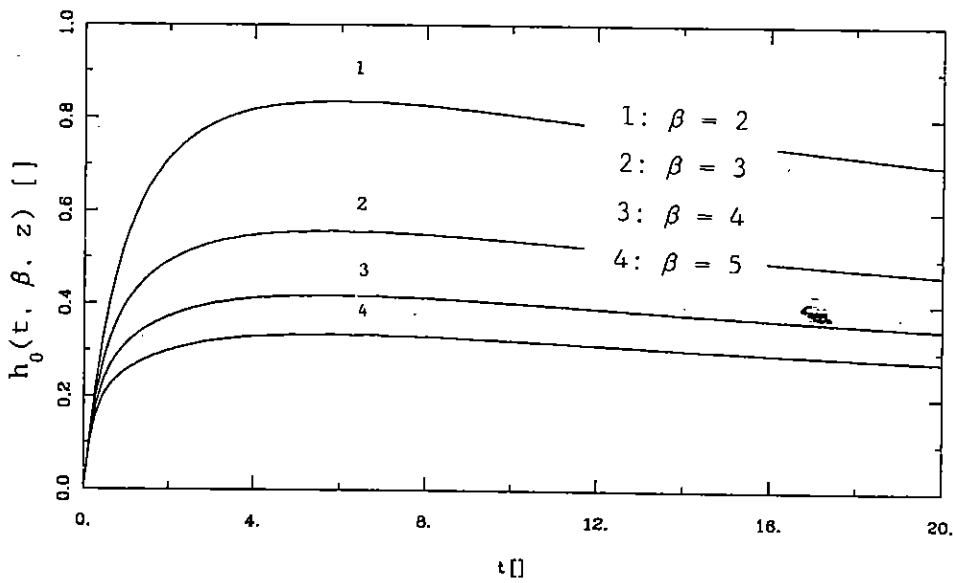
and where  $t'$  denotes the retarded time, which accounts for the propagation time delay, given by

$$t' = t - (\underline{x}_t \cdot \underline{r})/v. \tag{3.15}$$

In obtaining Eq.(3.13), we have also used the property  $f(at) = \mathcal{L}^{-1}\left(\frac{1}{a} \hat{f}\left(\frac{s}{a}\right)\right)$ .

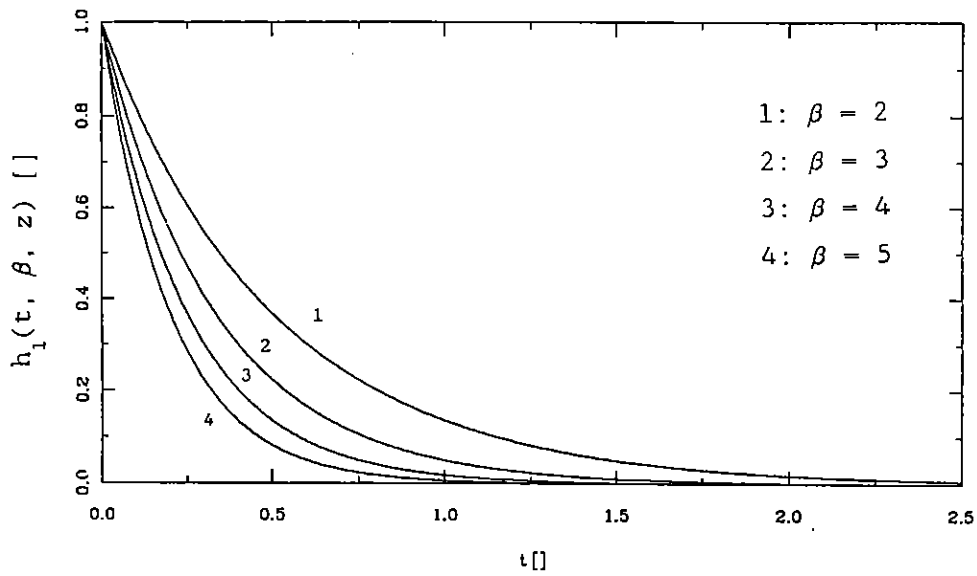


(a)

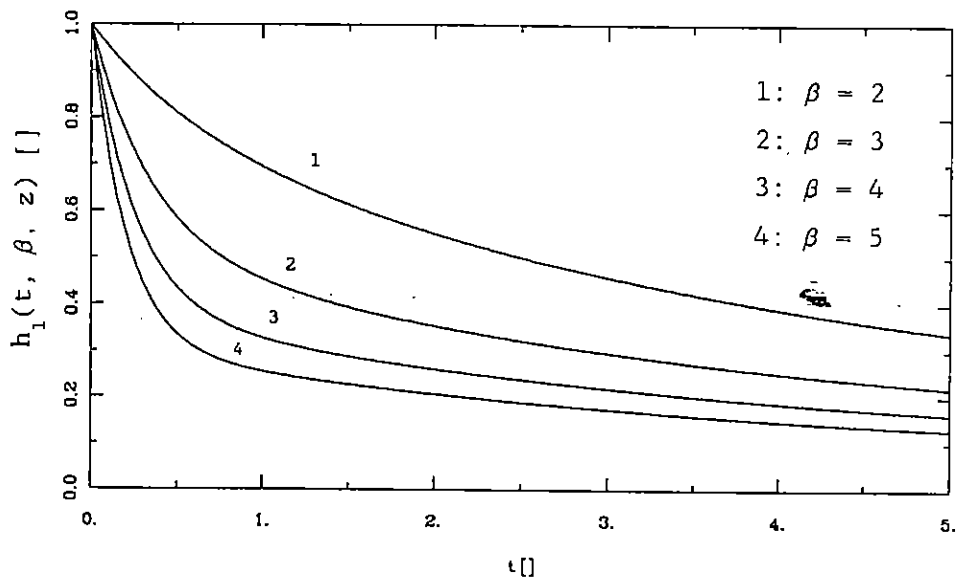


(b)

Fig. 3.2. The function  $h_0(t, \beta, z)$  as a function of time  
 a)  $z = 0$ ,  
 b)  $z = 3$ .



(a)



(b)

Fig. 3.3. The function  $h_1(t, \beta, z)$  as a function of time  
 a)  $z = 0$ ,  
 b)  $z = 3$ .



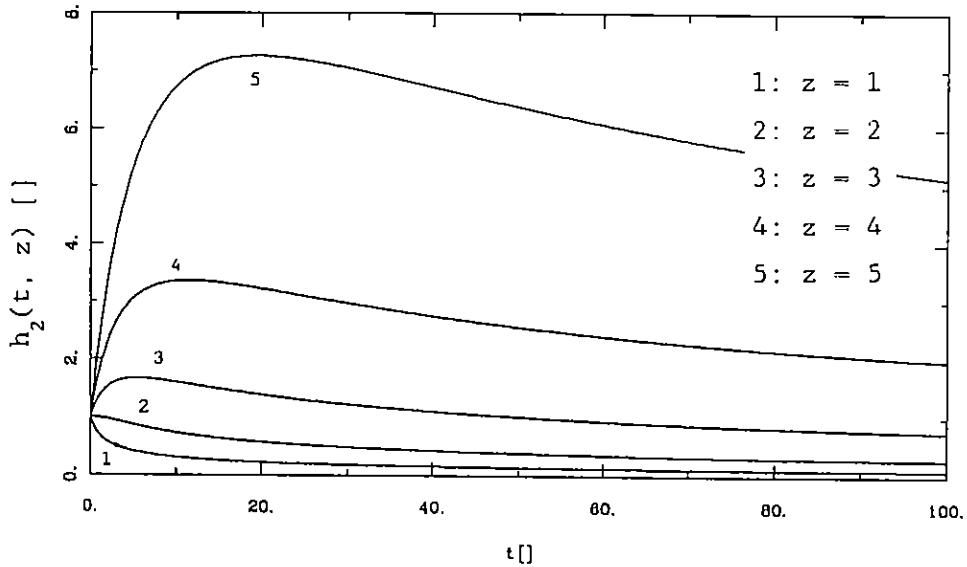


Fig. 3.4. The function  $h_2(t, z)$  as a function of time.

The transmitted wave is, of course, not a plane wave, but from the retarded time we can observe that the wave front propagates with speed  $v$ . Furthermore, the transmitted wave is attenuated by a factor  $e^{-z/\delta}$  while propagating in  $\mathcal{D}_2$ , and it depends only on  $at'$  and  $z'$ .

The values of the time-domain representation at  $t = 0$  and  $t = \infty$  can be found from the Laplace-domain expressions with Abel's theorem, which states that if the indicated limits exist, then

$$\lim_{s \rightarrow \infty} s \hat{f}(s) = \lim_{t \rightarrow 0} f(t),$$

$$\lim_{s \rightarrow 0} \hat{f}(s) = \lim_{t \rightarrow \infty} f(t).$$

(3.16)

When we apply the second identity of Abel's theorem to the Laplace-domain expression for the transmitted field given by Eq.(3.1), we find that for the late time the transmitted field approaches zero. But since the normalized Zenneck zero  $\xi$  can also become negative, it is not quite clear from

Eqs.(3.11)-(3.13) that it does. This topic is addressed in Appendix A, in which it is shown that for the late time any remaining non-vanishing terms cancel each other. So, the transmitted electric field approaches zero indeed under all conditions for the late time.

### 3.2 Transmitted magnetic fields

The transmitted magnetic fields in  $\mathcal{D}_2$  follow from Eq.(2.23) together with Eq.(2.24). The normal transmitted magnetic field is simply found to be

$$H_z^t(\underline{r}, t) = Y \sin \varphi_t E_y^t(\underline{r}, t), \quad (3.17)$$

where  $Y$  denotes the dielectric wave admittance of  $\mathcal{D}_2$  given by

$$Y = \sqrt{\epsilon/\mu}. \quad (3.18)$$

To derive a time-domain expression for the transverse transmitted magnetic field due to an incident unit-step function, we write

$$\hat{H}_x^t(\underline{r}, s) = -2 Y \cos \varphi_t s^{-1} \frac{\sqrt{s^2+2as}}{s + \rho\sqrt{s^2+2as}} \times e^{-s \frac{x}{v} \sin \varphi_t - \frac{z}{v} \cos \varphi_t \sqrt{s^2+2as}} \quad (3.19)$$

After multiplying the denominator as well as the numerator of Eq.(3.19) by  $\rho\sqrt{s^2+2as} - s$ , and again using the functions  $\hat{f}_0$  and  $\hat{f}_1$  defined by Eq.(3.12), Eq.(3.19) can be represented as

$$\hat{H}_x^t = -\frac{2}{\rho^2-1} Y \cos \varphi_t e^{-z'} e^{-\frac{s}{v}(\underline{x}_t \cdot \underline{r})} \left( \rho \left( 1 + \frac{2a}{s} \right) \frac{1}{a} \hat{f}_1 \left( \frac{s}{a}, \xi, z' \right) - \frac{1}{a} \hat{f}_0 \left( \frac{s}{a}, \xi, z' \right) \right). \quad (3.20)$$

This yields for the transverse magnetic field in the time domain

$$H_x^t(\underline{x}, t) = - \frac{2}{\rho^2 - 1} Y \cos \varphi_t U(t') e^{-z'} \left\{ \rho \left( 1 + 2a \int_0^{t'} d\tau \right) f_1(at', \xi, z') - f_0(at', \xi, z') \right\}. \quad (3.21)$$

Now, since

$$2a \int_0^{t'} f_1(ar, \lambda, z') dr = \frac{2}{\lambda} (f_1(at', 0, z') - f_1(at', \lambda, z')), \quad (3.22)$$

we finally obtain for the transverse magnetic field in the time domain

$$H_x^t(\underline{x}, t) = - \frac{2}{\rho^2 - 1} Y \cos \varphi_t U(t') e^{-z'} \left\{ \left[ f_1(at', \xi, z') + (\rho^2 - 1) f_1(at', 0, z') \right] / \rho - f_0(at', \xi, z') \right\}. \quad (3.23)$$

### 3.3 Reflected fields

The reflected fields propagate in the direction of  $\underline{\chi}_r$  given by

$$\underline{\chi}_r = \sin \varphi_i \underline{i}_x - \cos \varphi_i \underline{i}_z, \quad (3.24)$$

and can be found easily from the transmitted fields at the boundary. Since

$$\hat{R} = \hat{T} - 1, \quad (3.25)$$

we write directly in the time domain for the reflected electric field

$$E_y^r(\underline{r}, t) = E_y^t(z=0, t - (\underline{\chi}_r \cdot \underline{r})/c) - U(t - (\underline{\chi}_r \cdot \underline{r})/c), \quad (3.26)$$

which is a plane wave propagating in the direction of  $\underline{\chi}_r$ . The reflected magnetic fields follow simply from Eq.(2.11), and are found to be

$$H_x^r(\underline{r}, t) = \cos \varphi_i Y_0 E_y^r(\underline{r}, t),$$
$$H_z^r(\underline{r}, t) = \sin \varphi_i Y_0 E_y^r(\underline{r}, t). \quad (3.27)$$

#### 4 NUMERICAL RESULTS

In this Chapter, numerical results are presented for the scattering by a plane interface of a unit-step function and a Nuclear ElectroMagnetic Pulse (NEMP). In Section 4.1, some aspects about the numerical implementation are discussed.

##### 4.1 Numerical implementation

The expressions derived in the previous chapter are ready to be implemented in a computer program, except for the functions  $h_0$  and  $h_1$  given by Eq.(3.11). The most efficient implementation of the time-domain expressions uses a time-marching procedure, i.e., the fields at the time instant  $t+\Delta t$  are found from the fields at the time instant  $t$ , where  $\Delta t$  is the time step of the time-marching procedure. Consequently, we need to know  $h_0$  and  $h_1$  at the time instant  $t+\Delta t$  in terms of  $h_0$  and  $h_1$  at the time instant  $t$ . After some simple manipulation, we arrive at

$$\begin{aligned}
 h_0(t+\Delta t, \beta, z) = & e^{-\beta \Delta t} (h_0(t, \beta, z) \\
 & + e^{-\beta t} \int_t^{t+\Delta t} e^{-(1-\beta)\tau} I_0(\sqrt{\tau^2+2\tau z}) d\tau), \\
 h_1(t+\Delta t, \beta, z) = & e^{-\beta \Delta t} (h_1(t, \beta, z) \\
 & + z e^{-\beta t} \int_t^{t+\Delta t} e^{-(1-\beta)\tau} \frac{I_1(\sqrt{\tau^2+2\tau z})}{\sqrt{\tau^2+2\tau z}} d\tau).
 \end{aligned}
 \tag{4.1}$$

Numerical results are presented in the next sections. The integrals over the interval  $[t, t+\Delta t]$  were computed with an adaptive trapezoidal rule. The relative error in the total field solution as a result of the numerical integration is always less than 1%, independent of the time step  $\Delta t$ .

## 4.2 Unit-step incident field

The initial value of the fields can be found from the Laplace domain expressions using Abel's first identity of Eq.(3.16). From Eq.(3.1), we get

$$\lim_{t \rightarrow 0} E_y^t = \frac{2}{1+\rho}, \quad (4.2)$$

and so,

$$\lim_{t \rightarrow 0} E_y^r = \frac{1-\rho}{1+\rho}. \quad (4.3)$$

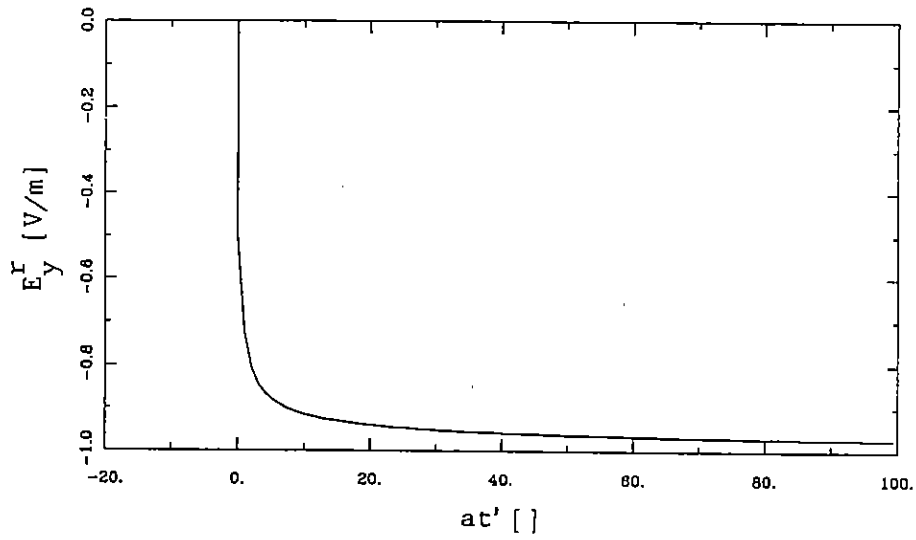
This result agrees with the time-domain equations (3.13) and (3.26).

Fig. 4.1 shows some results which were obtained from the time-domain expressions with  $\epsilon_r = 9$ ,  $\mu_r = 1$ ,  $\sigma = 1 \times 10^{-3}$  and the angle of incidence  $\varphi_i = 0$ . Consequently,  $E_y^t(\underline{r}=0, t=0) = 1/2$  and  $E_y^r(\underline{r}=0, t=0) = -1/2$ .

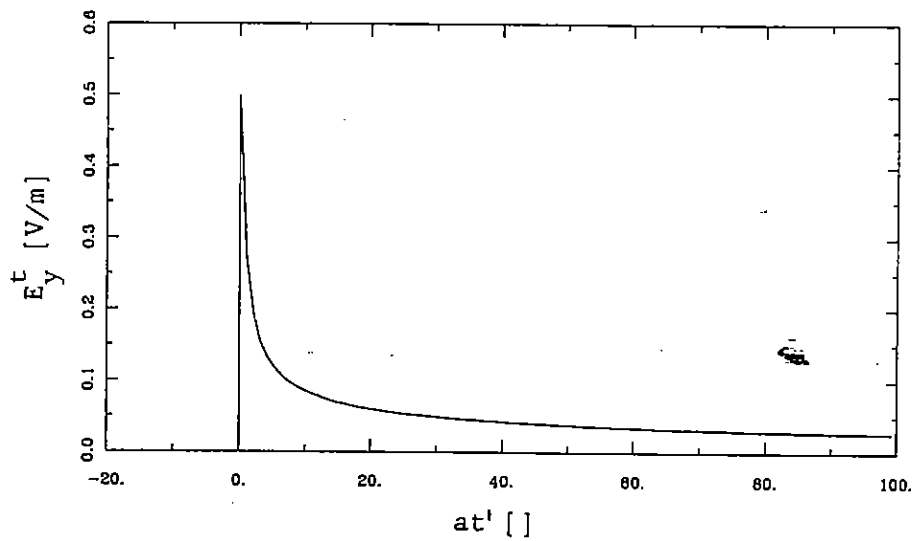
From Eq.(3.26) one can observe that the reflected field depends only on  $at'$  and  $\rho$ . Therefore, when  $\rho$  is kept constant and we vary the electrical conductivity  $\sigma$ , and thereby  $at'$ , only the time scale changes. Consequently, the rise time and half-width of the reflected fields vary inversely proportional with  $\sigma$ . Fig. 4.2 shows the reflected electric field for various  $\rho$  but with fixed  $\sigma$ . The rise time for any other electrical conductivity  $\sigma$  can be easily found from this figure in the following way. Select the curve with the correct  $\rho$ . Read the pertaining normalized rise time  $t'_r$ . The rise time for any other electrical conductivity  $\sigma$  is then determined from

$$t_r = \frac{2\epsilon_0 \rho^2 t'_r}{\sigma \cos^2 \varphi_i}. \quad (4.4)$$

The transmitted fields depend also on  $z/\delta$ , so a similar observation cannot be made. Fig. 4.3 shows the transmitted fields for  $\epsilon_r = 9$  and for different ratios of  $z/\delta$ .



(a)



(b)

Fig. 4.1 Electric field as a function of  $at'$ .  $\epsilon_r = 9$ ,  $\sigma = 1 \times 10^{-3}$ ,  
 $\mu_r = 1$ ,  $\varphi_i = 0$  and  $z = 0$ .  
 a) reflected field,  
 b) transmitted field.

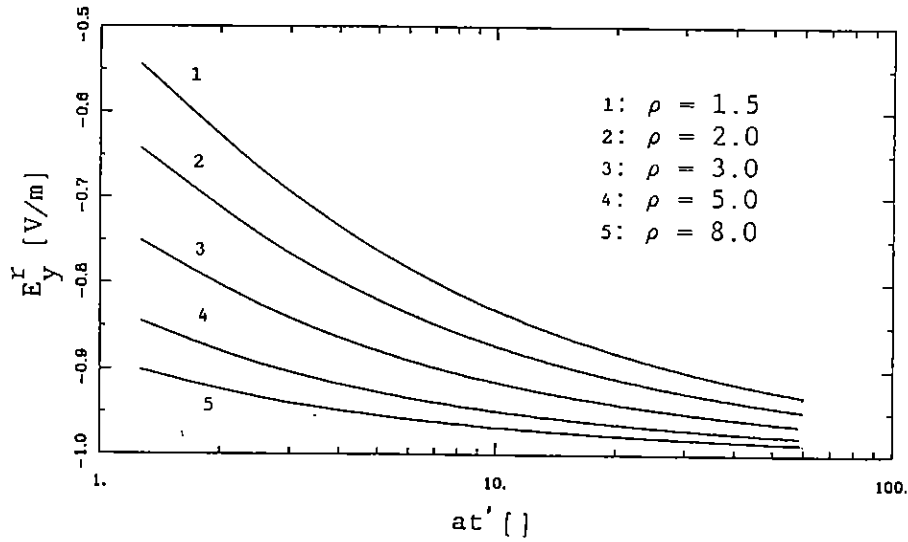


Fig. 4.2 Reflected electric field as a function of  $at'$  (logarithmic scale for clarity) and  $\rho$ . Electrical conductivity  $\sigma = 1 \times 10^{-3}$ .

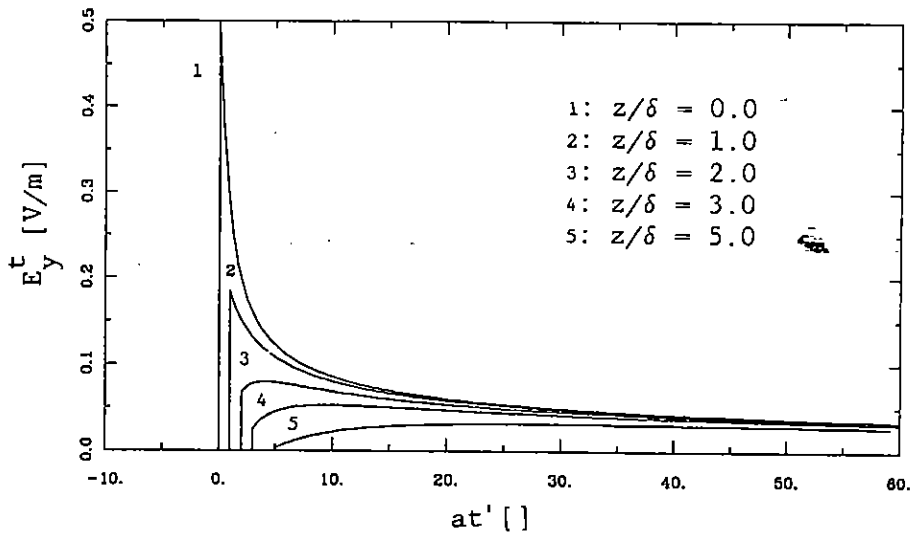


Fig. 4.3 Transmitted electric field as a function of  $at'$  for different ratios of  $z/\delta$ .  $\epsilon_r = 9$ ,  $\mu_r = 1$ ,  $\sigma = 1 \times 10^{-3}$ ,  $\varphi_i = 0$ .



### 4.3 NEMP incident field

In this Section results are presented for an incident Nuclear ElectroMagnetic Pulse (NEMP). The NEMP is a transient signal with a very-short rise time of about 5 ns and a large electric field strength with a peak value of 50 kV/m. The NEMP is approximated by a double exponential function given by (Bell laboratory waveform)

$$E_0(t) = A (e^{-\alpha t} - e^{-\beta t}) U(t), \quad (4.7)$$

with

$$\begin{aligned} A &= 5.278 \times 10^4 \quad \left[ \frac{V}{m} \right], \\ \alpha &= 3.705 \times 10^6 \quad [s^{-1}], \\ \beta &= 3.908 \times 10^8 \quad [s^{-1}]. \end{aligned} \quad (4.8)$$

The transmitted electric field due to a NEMP is obtained from the unit-step response in the way described in Appendix C. We then find from Eqs.(4.7), (3.13) and (C.8)

$$E_y^t(\underline{r}, t) = A(F(at', \beta/a, z') - F(at', \alpha/a, z')), \quad (4.9)$$

where

$$t' = t - (\underline{\chi}_t \cdot \underline{r})/v, \quad (4.10)$$

$$z' = z/\delta,$$

and where F is given by

$$F(t, \alpha, z) = \frac{2\alpha}{\rho^2 - 1} e^{-z} \int_0^t e^{-\alpha(t-\tau)} \left\{ \rho f_0(\tau, \xi, z) - f_1(\tau, \xi, z) \right\} d\tau. \quad (4.11)$$

In Eq.(4.11),  $\xi$  denotes the normalized Zenneck zero, given by

$$\xi = \frac{2\rho^2}{\rho^2 - 1}. \quad (4.12)$$

Now using the identities

$$\int_0^t e^{-\alpha(t-\tau)} h_0(\tau, \xi, z) d\tau = \frac{1}{\alpha-\xi} (h_0(t, \xi, z) - h_0(t, \alpha, z)),$$

$$\int_0^t e^{-\alpha(t-\tau)} h_1(\tau, \xi, z) d\tau = \frac{1}{\alpha-\xi} (h_1(t, \xi, z) - h_1(t, \alpha, z)), \quad (4.13)$$

$$\int_0^t e^{-\alpha(t-\tau)} h_2(\tau, z) d\tau = h_0(t, \alpha, z),$$

together with Eq.(3.12), F can be written as

$$F(t, \alpha, z) = \frac{2}{\rho^2 - 1} \frac{\alpha}{\alpha - \xi} e^{-z} \left( \begin{aligned} &\rho \left( (\alpha - 2)h_0(t, \alpha, z) - (\xi - 2)h_0(t, \xi, z) \right) \\ &+ h_1(t, \alpha, z) - h_1(t, \xi, z) \end{aligned} \right). \quad (4.14)$$

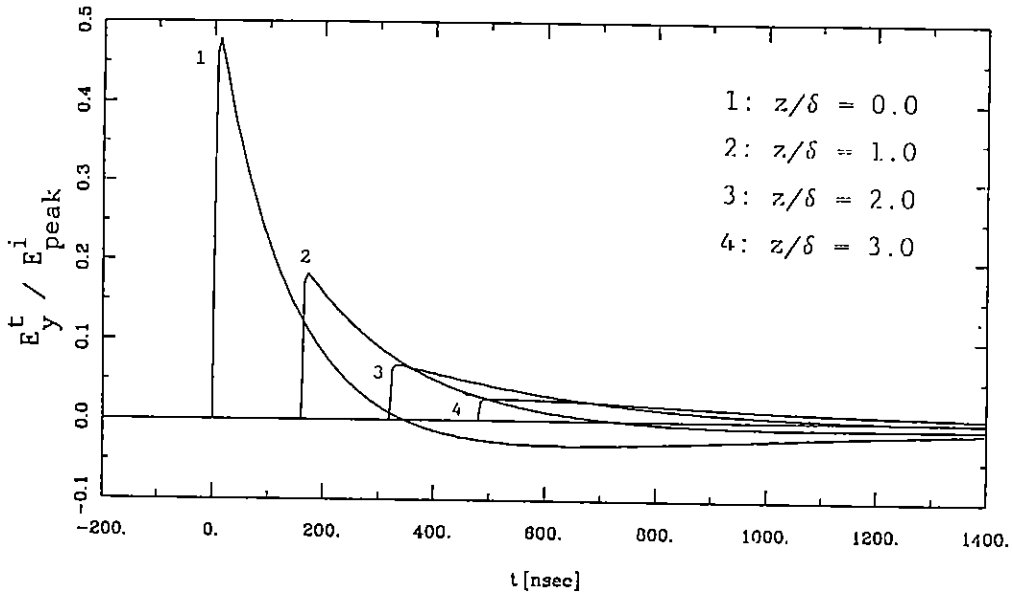
Obviously, the reflected electric field is then given by

$$E_y^R(\underline{r}, t) = A(F(at', \beta/a, 0) + e^{-\beta t'} - F(at', \alpha/a, 0) - e^{-\alpha t'}), \quad (4.15)$$

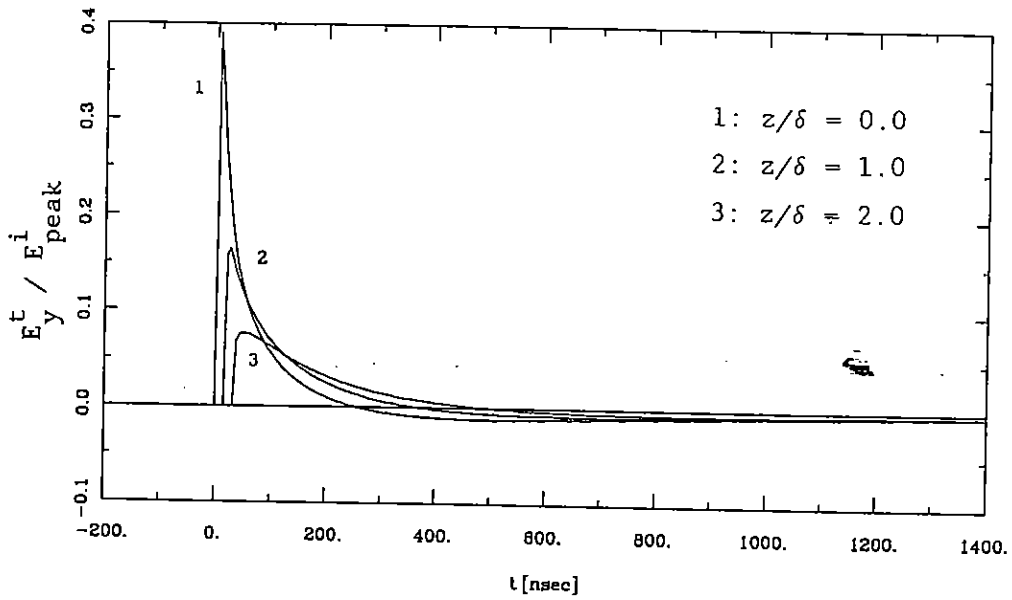
where the retarded time  $t'$  is now given by

$$t' = t - (\underline{x}_R \cdot \underline{r})/c_0. \quad (4.16)$$

Figs.4.4 and 4.5 show the transmitted and reflected NEMP, respectively, for  $\epsilon_r = 9$ ,  $\mu_r = 1$ ,  $\varphi_i = 0$ .



(a)



(b)

Fig. 4.4. Transmitted NEMP for different  $z$ .  $\epsilon_r = 9$ ,  $\mu_r = 1$ ,  $\varphi_i = 0$ .  
 a)  $\sigma = 1 \times 10^{-3}$ ,  
 b)  $\sigma = 1 \times 10^{-2}$ .

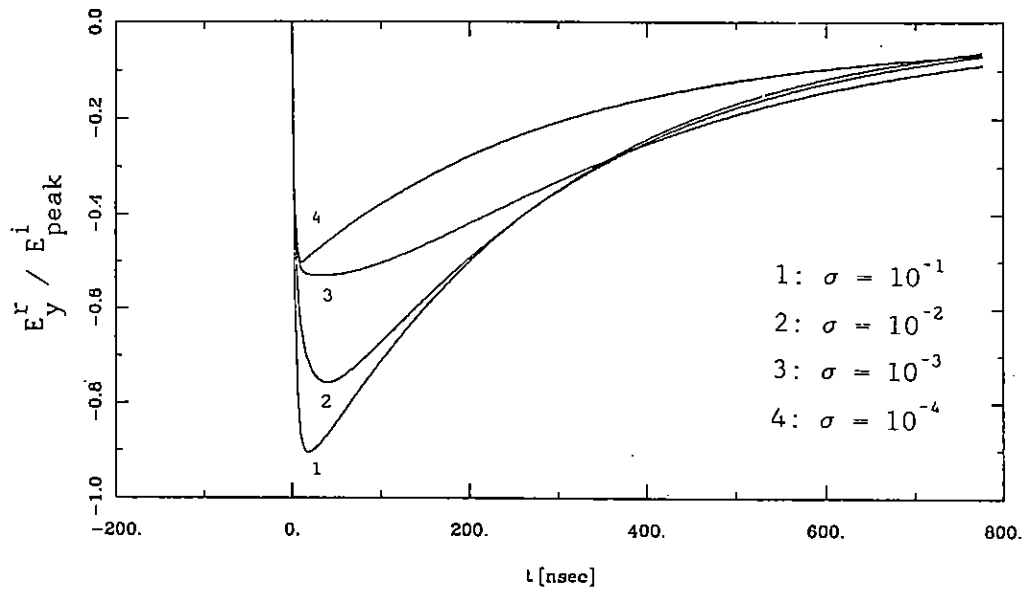


Fig. 4.5. Reflected NEMP for various electrical conductivity.  $\epsilon_r = 9$ ,  $\mu_r = 1$ ,  $\varphi_i = 0$ ,  $z = 0$ .

## 5 CONCLUSIONS

It was shown that time-domain expressions for the scattered electromagnetic fields due to a unit-step incident field, can be obtained from the Laplace-domain expressions. This Note investigated the case for horizontal polarization only. For vertical polarization the same procedure can be applied, Klaasen [3]. The time-domain expressions for vertical polarization are more complicated, because the reflection coefficient has two Zenneck zeros instead of one.

The scattered fields due to an incident field with a waveform other than the unit-step function, can be obtained from the derived unit-step responses. In Appendix C a method is presented for doing this. This method typically involves a convolution integral.

The presented time-domain expressions exhibit the useful property that in those cases where the waveform of the incident field  $f(t)$  can be written as  $f(t-\tau) = f_1(t)f_2(\tau)$ , the convolution can be determined very efficiently by a time-marching procedure. This is because the part  $f_1(t)$  can be taken outside the integral sign so that the integrand becomes time independent.

6 REFERENCES

- [1] *Barlow, H.M., Brown, J.,*  
Radio Surface Waves, Oxford University Press, 1962, pp. 29 - 45.
- [2] *Klaasen, J.J.A.,*  
Frequency-domain analysis of one-dimensional electromagnetic scattering by lossy media, Physics and Electronics Laboratory TNO (FEL-TNO) report FEL-90-A112, March 1990.
- [3] *Klaasen, J.J.A.,*  
Time-domain analysis of one-dimensional electromagnetic scattering by lossy media, Physics and Electronics Laboratory TNO (FEL-TNO) report FEL-90-A211, October 1990.
- [4] *Klaasen, J.J.A.,*<sup>1</sup>  
The late-time behavior of the one-dimensional electromagnetic field quantities, Physics and Electronics Laboratory TNO (FEL-TNO) report FEL-91-A015, January 1991.
- [5] *LePage, W.R.,*  
Complex Variables and the Laplace Transform for Engineers, McGraw-Hill Book Company, Inc., 1961, pp. 318 - 320.
- [6] *Leuthäuser, K.-D.,*  
Reflexion und Transmission von NEMP-Feldern, Bericht 120, Fraunhofer-Institut für Naturwissenschaftlich-Technische Trendanalysen (INT), July 1985, in German.
- [7] *Papoulis, A.,*  
Signal Analysis, McGraw-Hill Book Company, Inc., 1982, pp. 12 - 24, 101 - 138.
- [8] *Stratton, J.A.,*  
Electromagnetic Theory, McGraw-Hill Book Company, Inc., 1941, pp. 490 - 511.

---

<sup>1</sup> This report is an erratum to [3].

## APPENDIX A THE LATE-TIME BEHAVIOR OF THE FIELD QUANTITIES

In this Appendix the late-time behavior of the field quantities is investigated. Especially for certain conditions, it is not clear that the time-domain representations given in Chapter 3 have the proper late time behavior. These conditions are that  $\epsilon_r < \mu_r$  and that the angle of incidence  $\varphi_i$  is smaller than the Brewster angle  $\varphi_b$ . However, in this Appendix, it shows that for the late time and under all conditions the transmitted electric field approaches zero, and the reflected electric field -1. These results correspond with those found after applying Abel's theorem to Eq.(3.1).

The transmitted electric field is represented as (cf. Eq.(3.13))

$$E_y^t(\underline{x}, t) = \frac{2}{\rho^2 - 1} U(t') e^{-z'} \left\{ \rho f_0(at', \xi, z') - f_1(at', \xi, z') \right\}, \quad (\text{A.1})$$

with  $z' \in \mathbb{R}^+$ ,  $\xi$  given by Eq.(3.8), and (cf. Eq.(3.12))

$$\begin{aligned} f_0(t, \xi, z) &= h_2(t, z) + (2 - \xi)h_0(t, \xi, z), \\ f_1(t, \xi, z) &= h_1(t, \xi, z). \end{aligned} \quad (\text{A.2})$$

The functions  $h_0$ ,  $h_1$  and  $h_2$  in Eq.(A.2) are given by (cf. Eq.(3.11))

$$\begin{aligned} h_0(t, \xi, z) &= e^{-\xi t} \int_0^t e^{-(1-\xi)\tau} I_0(\sqrt{\tau^2 + 2\tau z}) d\tau, \\ h_1(t, \xi, z) &= e^{-\xi t} \left[ 1 + z \int_0^t e^{-(1-\xi)\tau} \frac{I_1(\sqrt{\tau^2 + 2\tau z})}{\sqrt{\tau^2 + 2\tau z}} d\tau \right], \\ h_2(t, z) &= e^{-t} I_0(\sqrt{t^2 + 2tz}). \end{aligned} \quad (\text{A.3})$$

For certain conditions the parameter  $\xi$  can become negative, because  $\rho$  can become smaller than one. These conditions are that  $\epsilon_r < \mu_r$  and  $\varphi_i < \varphi_b$ . For all other conditions,  $\xi$  is positive (larger than two to be exact). So, the late-time behavior of the field quantities must be determined bearing in

mind that  $\xi$  can be positive or negative.

To prove that the transmitted electric field approaches zero for all values of  $\xi$ , we will derive alternative representations for  $h_0$  and  $h_1$ , but first we deal with  $h_2$ . Combining the  $e^{-z}$  term which occurs in Eq.(A.1) with  $h_2$ , and using the asymptotic expansion for  $I_0((t^2 + 2tz)^{1/2})$ , it can easily be proved that  $e^{-z}h_2$  approaches zero for the late time. The alternative representations for  $h_0$  and  $h_1$  are derived from their Laplace-domain representations. Combining Eqs.(3.4) and (3.12), we write

$$\hat{h}_0(s, \xi, z) = \frac{1}{s + \xi} e^{-z(\sqrt{s^2 + 2s} - (s+1))} \frac{1}{\sqrt{s^2 + 2s}}, \quad (A.4)$$

$$\hat{h}_1(s, \xi, z) = \frac{1}{s + \xi} e^{-z(\sqrt{s^2 + 2s} - (s+1))}.$$

The functions  $h_0$  and  $h_1$  are obtained by applying the inverse Laplace transform according to Eq.(2.3). This integral is solved by applying Cauchy's residue theorem to the Bromwich contour. To do so, we first have to locate all poles and branch points of  $\hat{h}_0$  and  $\hat{h}_1$ . Both  $\hat{h}_0$  and  $\hat{h}_1$  have a simple pole at  $s = -\xi$  and branch points at  $s = 0$  and  $s = -2$ . The pole<sup>2</sup> is located either to the left of  $s = -2$  or to the right of  $s = 0$ , because either  $\xi > 2$  or  $\xi < 0$ . Fig. A.1 shows the path of integration along the Bromwich contour, and the location of the singularities and the branch points of  $\hat{h}_0$  and  $\hat{h}_1$  in the complex  $s$ -plane, in which  $s=p+iq$ . The contour  $C_\infty$  represents a semicircle with an infinite radius, while  $C_{Br}$  denotes the contour along a branch cut pertaining to  $(s^2+2s)^{1/2}$ . The branch cut ensures that this complex valued square root is single valued in the entire  $s$ -plane.

<sup>2</sup> Although  $\xi$  denotes the normalized Zenneck zero, it represents a pole for the functions  $h_0$  and  $h_1$



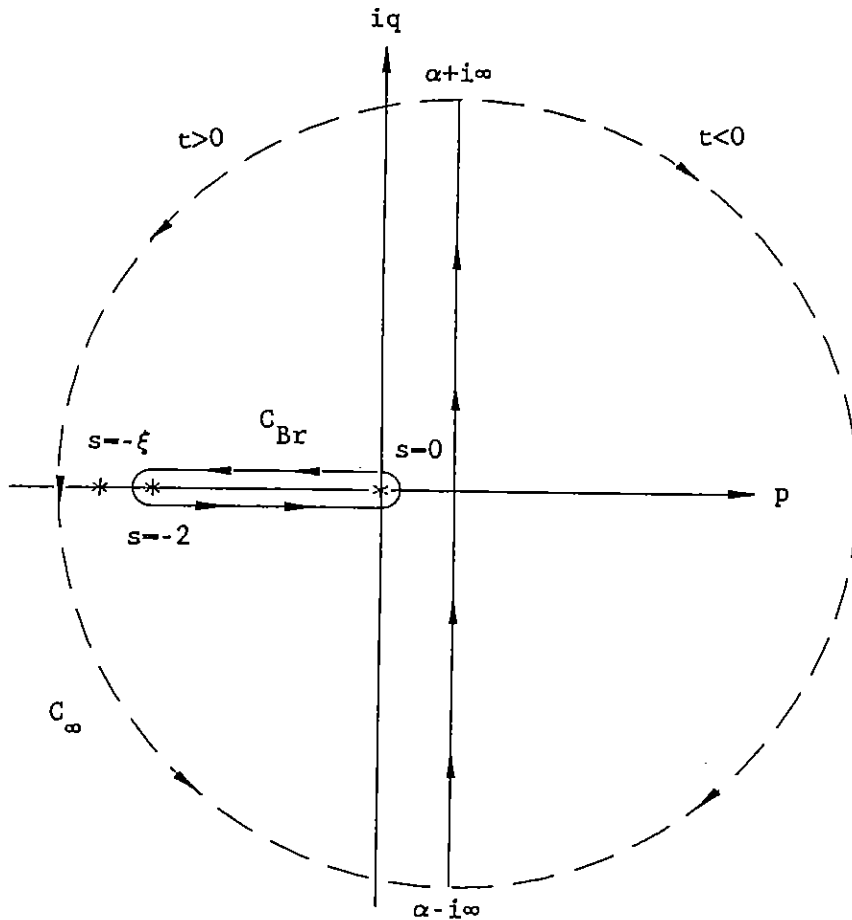


Fig. A.1. Location of the pole and branch points in the complex  $s$ -plane pertaining to the functions  $\hat{h}_0$  and  $\hat{h}_1$ .

Fig. 3.1 shows the behavior of  $(s^2+2s)^{1/2}$  in the complex  $s$ -plane with  $a = 1$ . To the right of the line  $s = -1$  the sign of  $\text{Re}((s^2+2s)^{1/2})$  is chosen positive. This ensures for  $t < 0$ , that the  $h_0(t) = 0$  and  $h_1(t) = 0$ . Note that the imaginary part of the root is positive in the upper half-plane, while it is negative in the lower half-plane.

For the time being let us focus on  $\hat{h}_1$ . Using Cauchy's residue theorem, we obtain

$$h_1 = \frac{1}{2\pi i} \left\{ \int_{C_{Br}} e^{st} \hat{h}_1 ds - \int_{C_\infty} e^{st} \hat{h}_1 ds \right\} + \text{Res}(e^{st} \hat{h}_1), \quad (\text{A.5})$$

where  $\text{Res}(\dots)$  denotes the residue at  $s = -\xi$ . It is a simple matter to prove with Jordan's lemma that the contribution from  $C_\infty$  vanishes for  $t > 0$ . The

contribution from the branch cut is

$$\frac{1}{2\pi i} \int_{C_{Br}} e^{st} \hat{h}_1 ds = \frac{e^{-t}}{2\pi i} \left\{ \int_1^{-1} \frac{1}{s+(\xi-1)} e^{st-z(i\sqrt{1-s^2}-s)} ds + \int_{-1}^1 \frac{1}{s+(\xi-1)} e^{st-z(-i\sqrt{1-s^2}-s)} ds \right\}, \quad (A.6)$$

where we have used the fact that the contributions from the semi-circles around the branch points vanish. After collecting terms, Eq.(A.6) can be rewritten as

$$\frac{1}{2\pi i} \int_{C_{Br}} e^{st} \hat{h}_1 ds = \frac{e^{-t}}{\pi} \int_{-1}^1 \frac{e^{s(t+z)}}{s+(\xi-1)} \sin(z\sqrt{1-s^2}) ds. \quad (A.7)$$

The residue contributes

$$\text{Res}(e^{st} \hat{h}_1) = e^{-\xi t - z((\xi-1) \pm \sqrt{\xi(\xi-2)})}, \quad (A.8)$$

where the plus sign has to be taken when the pole lies to the right of  $s = -1$ , and the minus when it lies to the left of  $s = -1$ . (see Fig.3.1). Finally, combining the Eqs.(A.7) and (A.8),  $h_1$  can be represented as

$$h_1 = \frac{e^{-t}}{\pi} \int_{-1}^1 \frac{e^{s(t+z)}}{s+(\xi-1)} \sin(z\sqrt{1-s^2}) ds + e^{-\xi t - z((\xi-1) \pm \sqrt{\xi(\xi-2)})}, \quad (A.9)$$

where the first term originates from the branch cut and the second term from the pole.

In a similar way, we find for  $h_0$

$$h_0 = \frac{e^{-t}}{\pi} \int_{-1}^1 \frac{e^{s(t+z)} \cos(z\sqrt{1-s^2})}{s+(\xi-1) \sqrt{1-s^2}} ds \pm \frac{e^{-\xi t - z((\xi-1) \pm \sqrt{\xi(\xi-2)})}}{\sqrt{\xi(\xi-2)}}, \quad (\text{A.10})$$

where the plus sign has to be taken when the pole lies to the right of  $s = -1$ , and the minus when it lies to the left of  $s = -1$ .

For the late time, the contribution from the branch cut to  $h_0$  and  $h_1$  approaches zero for all values of  $\xi$ , but the contribution from the pole approaches zero if  $\xi > 0$  only. So, for the late time the possible non-zero terms of the transmitted electric field are the contributions from the pole. Therefore, we write

$$E_y^t = \frac{2}{\rho^2 - 1} e^{-z'} \left\{ \pm \frac{\rho(2-\xi)}{\sqrt{\xi(\xi-2)}} e^{-a\xi t' - z'((\xi-1) \pm \sqrt{\xi(\xi-2)})} \right. \\ \left. - e^{-a\xi t' - z'((\xi-1) \pm \sqrt{\xi(\xi-2)})} \right\}. \quad (\text{A.11})$$

Using the expression for the Zenneck zero given by Eq.(3.8), this result can be rewritten as

$$E_y^t = - \frac{2}{\rho^2 - 1} e^{-z'} \left( \pm \frac{|\rho^2 - 1|}{\rho^2 - 1} + 1 \right) e^{-a\xi t' - z'((\xi-1) \pm \sqrt{\xi(\xi-2)})} \\ = 0 \quad \forall \rho \in \mathbb{R}. \quad (\text{A.12})$$

So, the contributions from the pole to the transmitted field cancel each other always. This is to be expected since the transmitted field does not exhibit a pole. Obviously, for the late time  $E_y^t(x, t)$  indeed approaches zero for all values of  $\xi$ . The late-time behavior of the reflected field follows from Eq.(3.26), and is found to approach -1. For the magnetic fields a similar proof can be given, but for brevity this will be omitted.

B STANDARD LAPLACE TRANSFORMS OF SOME BESSEL FUNCTIONS

$f(t)$	$\hat{f}(s)$
$I_0(at); t \geq 0$	$\frac{1}{\sqrt{s^2 - a^2}}$
$I_0(a\sqrt{t^2 + 2tb}); t \geq b \geq 0$	$\frac{1}{\sqrt{s^2 - a^2}} e^{-b(\sqrt{s^2 - a^2} - s)}$
$aI_1(at); t \geq 0$	$\frac{s}{\sqrt{s^2 - a^2}} - 1$
$\frac{ab}{\sqrt{t^2 + 2tb}} I_1(a\sqrt{t^2 + 2tb}); t \geq b \geq 0$	$e^{-b(\sqrt{s^2 - a^2} - s)} - 1$
$\frac{ab}{\sqrt{t^2 + 2tb}} I_1(a\sqrt{t^2 + 2tb}) + \delta(t); t \geq 0$	$e^{-b(\sqrt{s^2 - a^2} - s)}$
$\frac{at}{\sqrt{t^2 + 2tb}} I_1(a\sqrt{t^2 + 2tb}); t \geq b \geq 0$	$\left[ \frac{s}{\sqrt{s^2 - a^2}} - 1 \right] e^{-b(\sqrt{s^2 - a^2} - s)}$

C RESPONSE TO WAVEFORMS OTHER THAN THE UNIT-STEP FUNCTION

The impulse response of a linear system is the response of that system to a delta function excitation. Let the impulse response of such a system be denoted by  $h(t)$ . Then the response to an arbitrary input  $f(t)$  follows from the convolution theorem given by

$$g(t) = h(t) * f(t) = \int_0^t h(t-\tau)f(\tau) d\tau = \int_0^t h(\tau)f(t-\tau) d\tau, \quad (C.1)$$

where we have assumed that the system is causal, i.e.,  $h(t) = 0$  for  $t < 0$ , and that  $f(t) = 0$  for  $t < 0$ .

For the purpose of the derivation, we rewrite Eq.(C.1) as follows

$$g(t) = \int_{-\infty}^{\infty} h(\tau)U(\tau) f(t-\tau)U(t-\tau) d\tau, \quad (C.2)$$

where  $U(t)$  denotes the Heaviside unit-step function given by

$$U(t) = \begin{cases} 0 & t < 0 \\ 1 & t > 0 \end{cases} \quad (C.3)$$

Now, let  $w(t)$  denote the response to a unit-step function. Then  $w(t)$  can be obtained from the impulse response by

$$w(t) = \int_{-\infty}^{\infty} h(\tau)U(\tau) U(t-\tau) d\tau = \int_{-\infty}^t h(\tau)U(\tau) d\tau. \quad (C.4)$$

Observe from Eq.(C.4) that  $\partial_t w(t) = h(t) U(t)$ . Therefore, Eq.(C.2) can be rewritten as

$$g(t) = \int_{-\infty}^{\infty} \partial_{\tau} w(\tau) f(t-\tau)U(t-\tau) d\tau, \quad (C.5)$$

which yields after partial integration

$$g(t) = \int_{-\infty}^{\infty} w(\tau) \partial_t (f(t-\tau)U(t-\tau)) d\tau. \quad (C.6)$$

Now, using the identity

$$\partial_t (f(t)U(t)) = f'(t)U(t) + f(t)\delta(t), \quad (C.7)$$

where the prime denotes differentiation with respect to the argument of the function, Eq.(C.6) can be rewritten as

$$g(t) = w(t)f(0) + \int_0^t w(\tau)f'(t-\tau) d\tau = w(t)f(0) + w(t) * f'(t). \quad (C.8)$$

Eq.(C.8) gives the system response to any arbitrary input  $f(t)$  in terms of the unit-step response  $w(t)$ .